



# University of HUDDERSFIELD

## University of Huddersfield Repository

Hüe, F., Rodenburg, J., Maiden, A., Sweeney, Francis and Midgley, P.

Wave-front phase retrieval in transmission electron microscopy via ptychography

### Original Citation

Hüe, F., Rodenburg, J., Maiden, A., Sweeney, Francis and Midgley, P. (2010) Wave-front phase retrieval in transmission electron microscopy via ptychography. *Physical Review B*, 82 (12). ISSN 1098-0121

This version is available at <http://eprints.hud.ac.uk/id/eprint/16058/>

The University Repository is a digital collection of the research output of the University, available on Open Access. Copyright and Moral Rights for the items on this site are retained by the individual author and/or other copyright owners. Users may access full items free of charge; copies of full text items generally can be reproduced, displayed or performed and given to third parties in any format or medium for personal research or study, educational or not-for-profit purposes without prior permission or charge, provided:

- The authors, title and full bibliographic details is credited in any copy;
- A hyperlink and/or URL is included for the original metadata page; and
- The content is not changed in any way.

For more information, including our policy and submission procedure, please contact the Repository Team at: [E.mailbox@hud.ac.uk](mailto:E.mailbox@hud.ac.uk).

<http://eprints.hud.ac.uk/>

## Wave-front phase retrieval in transmission electron microscopy via ptychography

F. Hübner,<sup>1,\*</sup> J. M. Rodenburg,<sup>2</sup> A. M. Maiden,<sup>2</sup> F. Sweeney,<sup>2</sup> and P. A. Midgley<sup>1</sup>

<sup>1</sup>Department of Materials Science and Metallurgy, University of Cambridge, Pembroke Street, Cambridge CB2 3QZ, United Kingdom

<sup>2</sup>Department of Electrical and Electronic Engineering, University of Sheffield, Mappin Street, Sheffield, S1 3JD, United Kingdom

(Received 14 June 2010; published 24 September 2010)

There are many different strategies that allow the solving of the well-known phase problem corresponding to the loss of phase information during a physical measurement. In microscopy, and, in particular, in transmission electron microscopy, most of these strategies focus on the retrieval of high-resolution information with the importance of lower resolution data often overlooked. Ptychography offers a means to investigate such data. Ptychography is a robust diffractive imaging technique with fast convergence for phase retrieval but, until now, has not been applied at the nanoscale. In this paper, we use the ptychographical iterative engine to retrieve the phase change at the exit plane of metallic nanoparticles using a conventional transmission electron microscope. Ptychographical reconstructions yielded images with a phase resolution of  $\pi/10$  and a spatial resolution of 1 nm. These results stand as a first step toward aberration-free lensless imaging. The technique lends itself to be an alternative to off-axis electron holography or focal series reconstruction.

DOI: [10.1103/PhysRevB.82.121415](https://doi.org/10.1103/PhysRevB.82.121415)

PACS number(s): 68.37.Lp

A very long-standing issue in transmission electron microscopy (TEM) has been how to measure accurately the phase of the electron wave emanating from the exit surface of the specimen. Because the wavelength of an electron is reduced as it passes through a potential well, the atomic potentials within the specimen can induce significant changes in its phase relative to its free-space propagation. Measurement of the induced phase change at the atomic scale or nanoscale has many important applications: for example, the measurement of the mean inner potential in materials (which depends upon the local chemical distribution<sup>1</sup>), the measurement of magnetic fields around nanostructures,<sup>2</sup> or the measurement of internal electric fields within the specimen (e.g., at semiconductor junctions<sup>3</sup>).

Traditional TEM phase contrast is based upon an approximate version of Zernike's method<sup>4</sup> for thin and weakly scattering specimen. In essence, an interference image is created by adding the unscattered and phase-modified scattered terms. The resulting contrast is then a combination of amplitude and phase components. The transfer function of the lens is a serious limitation of this method, especially at low scattering angles (low-resolution components in the image), meaning that phase contrast works well only for relatively small-scale features, below about 1.0 nm. Furthermore, the weak-scattering approximation breaks down for all but the thinnest (few nanometers), light-element specimens.

One technique that overcomes some of these limitations requires the recording of two or more images at different defoci of the objective lens, thus imaging a number of planes downstream of the object. As a wave propagates, only one phase distribution will be consistent with the measured changes of intensity. There are several methods for retrieving phase using such data.<sup>5–8</sup> However, because the wave intensity relies on local interference between wavelets in the Fresnel propagation integral, then—such as the bright-field image—it is also poor at measuring quantitative large-scale phase distributions across a wide field of view. To date, the only method for capturing large phase changes which also have large-scale features over a significant field of view ( $\sim 1 \mu\text{m}$ ) is off-axis electron holography.<sup>9,10</sup> This, though,

requires demanding experimental stability for the interfering beams and conventionally there must be an area of free space adjacent to the feature of interest in order to create a true reference wave (i.e., where the phase of the electron wave does not change as the wave propagates). There are also extremely high demands on the coherence of the illuminating beam.

A completely different approach to the image phase problem is to solve for the phase of the diffraction pattern scattered by the object, and then computationally backpropagate this to the object plane—so-called coherent diffractive imaging (CDI). Solution of the diffraction phase problem is via iterative phase-retrieval algorithms, originally inspired by the work of Gerchberg and Saxton.<sup>11</sup> When *a priori* information about the shape or extent of the object is known, the principle of oversampling the diffracted intensity can be used to provide a solution of the phase problem from a single diffraction pattern alone.<sup>12,13</sup> However, most of the proposed algorithms—error reduction,<sup>11</sup> hybrid input-output,<sup>14</sup> charge flipping,<sup>15</sup> difference map<sup>16</sup>—require not only the diffracted intensities but also some knowledge of the extent of the (finite) object. CDI has been shown to work for weakly scattering objects over a limited field of view in electron microscopy.<sup>17</sup> Different groups have also shown that it is possible to converge toward a good solution for extended objects with the use of a strong support.<sup>18,19</sup>

In this Rapid Communication we demonstrate experimentally a method of accurately imaging large phase changes ( $> \pi$ ) in the electron exit wave induced by objects of unlimited lateral dimensions for which there is no *a priori* information. The technique, called ptychography,<sup>20–23</sup> was first proposed by Hoppe in 1969 (Ref. 24) as a solution to the crystalline phase problem, wherein an aperture or a confined beam of illumination is moved over the specimen while multiple diffraction patterns are recorded from overlapping regions of the specimen. Nellist *et al.*<sup>20</sup> demonstrated this method for the case of a crystalline specimen. Since then, an iterative phase-retrieval algorithm, based on the same concept of a back and forward Fourier transform iteration procedure used in CDI methods [Fig. 1(b)], has been developed

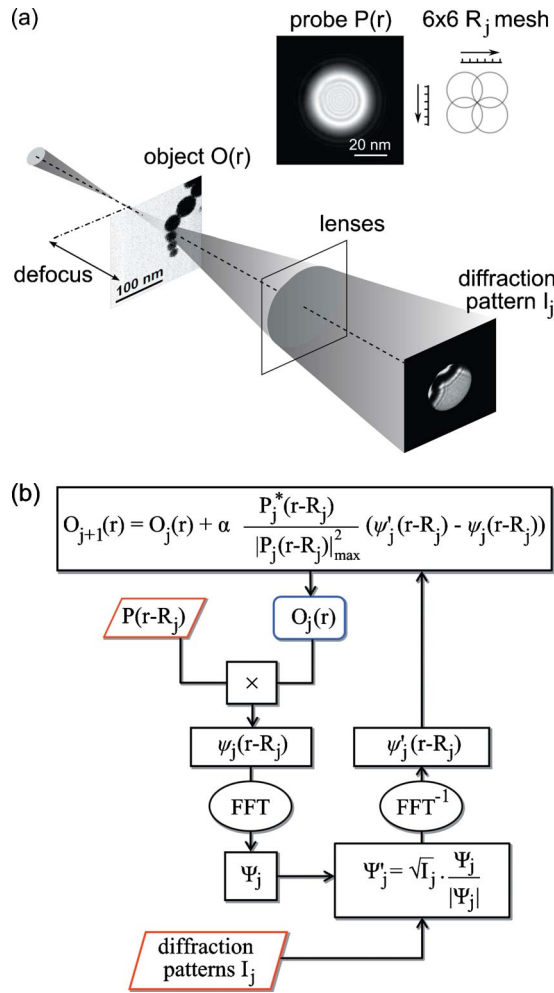


FIG. 1. (Color online) (a) Schematic representation of the setup in TEM and (b) ptychographic reconstruction flowchart using the PIE. The PIE algorithm uses the illumination function, probe  $P(r)$ , its positions  $R_j$  and the corresponding diffraction patterns to retrieve the unknown object function  $O(r)$ . With  $\psi$  the exit wave function,  $\Psi$  its Fourier transform, and  $I_j$  the recorded intensities in the diffraction plane for each  $R_j$  position of the probe  $P(r-R_j)$  relative to the object  $O(r)$ .  $\alpha$  is a feedback parameter.

which exploits nonperiodic ptychographical data. This has the benefits of removing the stagnation problems that can occur for complex-valued object functions using conventional iterative methods, greatly speeding up convergence to the solution of the phase problem and allowing objects of unlimited size to be imaged. The technique has previously shown excellent results using both visible light<sup>25</sup> and hard X-rays.<sup>26,27</sup> We show that electron ptychography of large-scale (200 nm) features can measure phase changes with about the same accuracy as off-axis holography but without the need for a stable reference wave and an area of free space adjacent to the area of interest.

The test specimen was a  $\text{Fe}_{0.3}\text{Ni}_{0.7}$  powder prepared by cryogenic evaporation/condensation, used previously for magnetic studies.<sup>2</sup> Produced by rapid vapor condensation, these alloys have typical grain sizes of 50 nm coated with 3 nm of oxide. If the objective lens is energized, this ferromagnetic specimen becomes magnetically saturated parallel

to the optical axis. In such circumstances, the phase shift recorded is due only to the electrostatic potential. Away from strongly diffracting orientations and in the absence of stray electric field, the phase shift will be proportional to the mean inner potential (MIP).

TEM ptychography observations were performed on a FEI Tecnai F20, a field-emission gun TEM (FEGTEM) fitted with a Gatan  $1024 \times 1024$  pixel charge-coupled-device (CCD) camera and an on-axis Fischione Model 3000 high-angle annular dark-field (HAADF) detector for high-resolution scanning TEM (STEM) imaging. The experimental conditions were chosen to have a low electron density at each probe position to minimize the dose on the specimen and possible contamination. We used FEI TIA® software to control accurately the probe movement in STEM microprobe mode. The convergence semiangle was 1.42 mrad and the probe was overfocused by  $14 \mu\text{m}$  [defocus in Fig. 1(a)] in order to have a probe of diameter 40 nm in the focal plane of the objective lens. The diffraction patterns were recorded on the camera located after the Gatan imaging filter (GIF) with a nominal camera length of 40 mm (for the HAADF detector). In our system, the recorded diffraction patterns are in essence, like previous single-shot recordings,<sup>9,28,29</sup> inline Fraunhofer holograms. Unlike inline holography however, ptychography allows the unambiguous reconstruction of the exit-plane wave without the “twin-image” problem brought about by the complex conjugate solution. The exposure time was 1 s at each position,  $R_j$ . The optimized illumination conditions for our microscope (Tecnai F20) were: gun lens 5, extraction 3800 V, spot size 10. Redundancy in the data, needed for ptychographic applications, was enforced with a scanning step size small enough for adjacent views to overlap. For the best results the overlap (relative to the diameter of the probe) has to be around 70% (Ref. 30) but should not exceed 85% (Ref. 31), we chose an overlap of 76% with a calibrated probe step of 9.5 nm and a probe diameter of 40 nm.

Figure 1(a) shows a simplified path of the electron wave front in a TEM from the demagnified virtual source to the diffraction plane. The defocus creates a convergent incident beam onto the specimen in real space. This beam is moved across the specimen and intensities are recorded in the reciprocal plane (Fourier plane) for each specified position of the probe ( $R_j$ ). The ptychographical iterative engine (PIE) algorithm<sup>22</sup> enables the reconstruction of the wave function in the object plane from the recorded intensities in reciprocal space. The PIE needs only the complex probe function and the probe positions relative to the object to retrieve the phase and amplitude of the exit wave front. In our case, the illumination function probe— $P(r)$  in Fig. 1(a)—is determined by an inverse Fourier transform of a diffraction pattern recorded in the vacuum with a phase calculated from the defocus and the spherical aberration of the objective lens. At each iteration of the PIE algorithm, diffraction patterns recorded at the  $R_j$  positions are considered successively and are used to update the amplitude of the Fourier transform of the exit wave. Feedback parameter  $\alpha$  conditions the speed of convergence and the changes occurring between two successive iterations.<sup>30</sup>

The major unforeseen difficulty we encountered was to

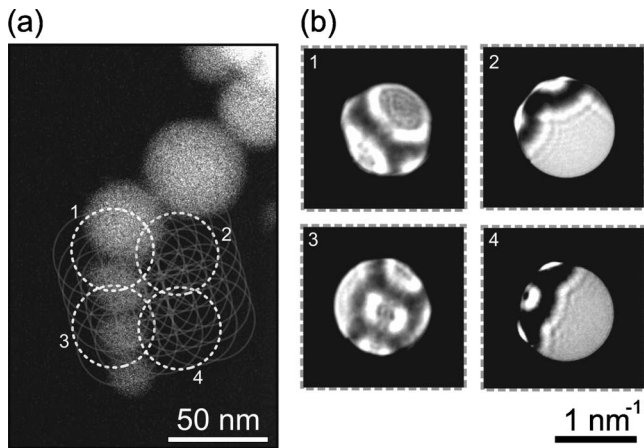


FIG. 2. Experimental recordings for  $\text{Fe}_{0.3}\text{Ni}_{0.7}$  particles. (a) STEM HAADF image, where the circles indicate the 36 probe positions for which diffraction patterns were recorded. (b) Central disks of diffraction patterns for the positions indicated by dotted circles in (a).

determine the actual probe positions. As a first step, probe positions were estimated by knowing the step incremented in TIA. Nevertheless, hysteresis and specimen drift force us to correct each position by an inverse Fourier transform of the recorded diffraction patterns (using the phase of the probe as a first approximation). This refinement is essential and leads to the true probe positions. Thus a regular grid (typically rhombus shaped) was defined for the  $j$  positions of the probe. Figure 2 represents this grid relative to a STEM HAADF image of our specimen. PIE was used to compute the exit wave function for 1000 iterations with a feedback parameter  $\alpha$  of 1. A defocused probe on the specimen has two principal advantages: a low dose exposure of the specimen and an unsaturated central peak on the 14-bit CCD camera for a 1 s acquisition. The camera length was chosen very carefully relative to the probe size (driven by defocus and convergent semiangle). In our case, a nominal camera length of 40 mm allowed us to have a real-space field of view of 93 nm (maximum) which is close to ideal for the reconstruction of a 40 nm probe without loss of information.

We compared the phase images obtained by ptychographical reconstruction with those by off-axis holography. Off-axis electron holograms were acquired at 300 kV using a Philips CM300ST FEGTEM equipped with an electrostatic Möllenstedt biprism, a GIF, and a  $2048 \times 2048$  pixel CCD camera (Gatan). We recorded holograms from  $\text{Fe}_{0.3}\text{Ni}_{0.7}$  nanoparticles of the same specimen previously studied by ptychography. The illumination conditions were set to maximize the visibility (degree of coherence) of the holographic fringes. In our case, the visibility was 18% with a fringe spacing of 0.25 nm. Due to the shot noise of the detector, the theoretical smallest phase difference we are able to discern (for integrated area of  $1 \text{ nm} \times 1 \text{ nm}$ ) is 0.3 rad.<sup>32</sup>

Most CDI experiments in the literature show excellent qualitative results but very few are quantitative. Here we compare directly and quantitatively ptychography with off-axis holography. Figure 3 shows the comparison of these two techniques: ptychography with PIE running for 1000 itera-

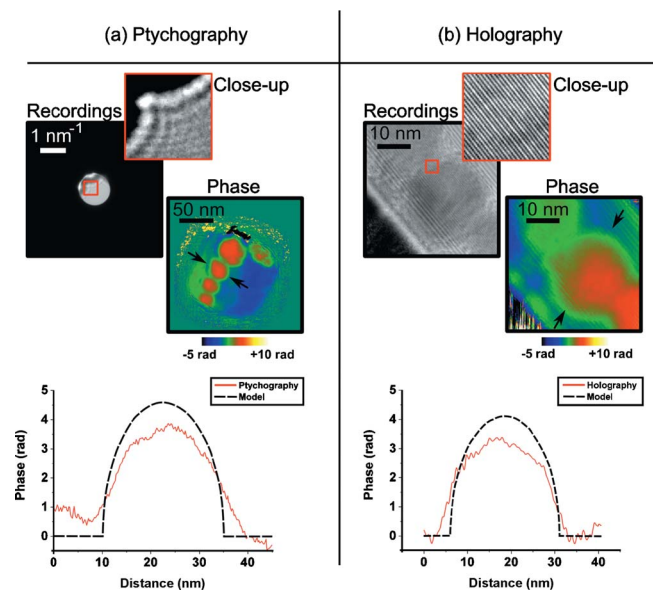


FIG. 3. (Color online) Quantitative phase retrieval for spherical particles of  $\text{Fe}_{0.3}\text{Ni}_{0.7}$ , (a) by electron ptychography running the PIE for 1000 iterations and (b) by off-axis holography. In both cases, a phase profile through a 25 nm particle (plane lines) is compared with a theoretical profile for a perfectly spherical particle (dashed lines).

tions, Fig. 3(a), and off-axis holography, Fig. 3(b). In both cases, a profile has been taken through the center of a 25 nm particle. As no stray electric field or magnetization is relevant in this simple case, the measured phase is a topographic profile proportional to the projected MIP of the particle. In the case of a spherical  $\text{Fe}_{0.3}\text{Ni}_{0.7}$  particle, and assuming that the MIP is constant within the specimen, the theoretical induced phase shift due to the thickness should reach a maximum of 4.6 rad and 4.1 rad for 200 and 300 keV, respectively (with the free electron contribution taken into account<sup>1</sup>). In both cases, the phase measurement (3.9 rad for ptychography at 200 keV and 3.1 rad for holography at 300 keV) underestimates this maximum value, as shown with the profile lines in Fig. 3. This result is not a surprise as the MIP of the sphere is actually a measurement of both its core and its overlayer. We performed simulations to quantify the reliability of ptychography with regard to the different factors of error (probe position, phase jump, and diffraction pattern centering). By far, the biggest source of error is the accuracy of the probe positioning. We calculated the phase precision to be 0.3 rad in the case of a probe position uncertainty of 0.5 nm. This estimation is in good agreement with the noise of the phase calculated in the free-space area next to the  $\text{Fe}_{0.3}\text{Ni}_{0.7}$  particles. The PIE converged to a quantitative consistent solution for the phase in less than 1000 iterations. The variation in the phase observed in the free space is certainly due to a residual probe position error.

Unlike off-axis holography, ptychography retrieves the value of the phase shift without the need for a reference wave. Such a phase measurement is of great use for particles supported on carbon film or embedded in resin. Another advantage of ptychography compared to off-axis holography is that the latter technique requires high coherence, a biprism

near the image plane and an additional objective mini lens for low-resolution observation ( $\sim 1 \mu\text{m}$  field of view).<sup>10</sup> In comparison, in ptychography a large field of view can be reached by simply increasing the number of probe positions.

We demonstrate electron ptychography of a nonperiodic object, showing that it is able to retrieve strong phase change induced by thick samples over a wide field of view. Although through-focal series<sup>7,33</sup> and off-axis electron holography can be used for reconstructing the electron exit wave phase and modulus, the unique potential of ptychography is that, being a CDI technique, it should not ultimately be dependent upon a good-quality imaging lens, and so could be developed to retrieve image information at much higher resolution than currently available. Until now, one of the most stringent limitations of CDI methods has been the need for isolated objects (the so-called support constraint). Ptychography works without this support constraint and is able to solve the phase problem for extended objects. Drift remains one of the main limitations of the technique: typical experiment duration for 36 probe positions is about 2 min, in which the object can

drift 1–2 nm depending of the holder and the microscope environment. At the moment, drift prevents subnanometer accuracy (unlike single-shot acquisition<sup>34</sup>). For a spatial resolution of 1 nm, partial coherence in convergent illumination ( $\sim 1.5 \text{ mrad}$ ) is not a limiting factor.

Parallel illumination would avoid the problem of any variation in diffraction contrast when rastering a convergent probe but it would require a single camera with a very high dynamical range, one with a less sensitive part for the central peak or a radiation-hardened direct electron detection camera. A remote-controlled piezoholder or a movable selected-area aperture could be a perspective of future research. The driving ambition of this research is for lens-free systems, avoiding the problem of lens aberrations such that spatial resolution is only diffraction limited.

Yannick Champion is acknowledged for providing the  $\text{Fe}_{0.3}\text{Ni}_{0.7}$  powder. This work was funded by the EPSRC Basic Technology under Grant No. EP/E034055/1 in the framework Pi-Phi project.

\*Corresponding author; fmh29@cam.ac.uk

<sup>1</sup>M. Gajdardziska-Josifovska and A. H. Carim, *Introduction to Electron Holography*, edited by E. Völkl (Kluwer Academic/Plenum, New York, 1999).

<sup>2</sup>M. J. Hytch, R. E. Dunin-Borkowski, M. R. Scheinfein, J. Moulin, C. Duhamel, F. Mazaleyrat, and Y. Champion, *Phys. Rev. Lett.* **91**, 257207 (2003).

<sup>3</sup>A. C. Twitchett, R. E. Dunin-Borkowski, and P. A. Midgley, *Phys. Rev. Lett.* **88**, 238302 (2002).

<sup>4</sup>F. Zernike, *Physica (Amsterdam)* **9**, 686 (1942).

<sup>5</sup>D. L. Misell, R. E. Burge, and A. H. Greenaway, *J. Phys. D* **7**, L27 (1974).

<sup>6</sup>W. Coene, G. Janssen, M. Op de Beeck, and D. Van Dyck, *Phys. Rev. Lett.* **69**, 3743 (1992).

<sup>7</sup>D. van Dyck and A. F. de Jong, *Ultramicroscopy* **47**, 266 (1992).

<sup>8</sup>H. W. Zandbergen, R. Bokel, E. Connolly, and J. Jansen, *Micron* **30**, 395 (1999).

<sup>9</sup>A. Tonomura, *Rev. Mod. Phys.* **59**, 639 (1987).

<sup>10</sup>H. Lichte, P. Formanek, A. Lenk, M. Linck, C. Matzeck, M. Lehmann, and P. Simon, *Annu. Rev. Mater. Res.* **37**, 539 (2007).

<sup>11</sup>R. W. Gerchberg and W. O. Saxton, *Optik (Stuttgart)* **35**, 237 (1972).

<sup>12</sup>D. Sayre, *Acta Crystallogr.* **5**, 843 (1952).

<sup>13</sup>J. Miao, T. Ishikawa, E. H. Anderson, and K. O. Hodgson, *Phys. Rev. B* **67**, 174104 (2003).

<sup>14</sup>J. R. Fienup, *Appl. Opt.* **21**, 2758 (1982).

<sup>15</sup>G. Oszlányi and A. Sütő, *Acta Crystallogr., Sect. A: Found. Crystallogr.* **A60**, 134 (2004).

<sup>16</sup>V. Elser, *J. Opt. Soc. Am. A Opt. Image Sci. Vis* **20**, 40 (2003).

<sup>17</sup>J. M. Zuo, I. Vartanyants, M. Gao, R. Zhang, and L. A. Nagahara, *Science* **300**, 1419 (2003).

<sup>18</sup>W. J. Huang, J. M. Zuo, B. Jiang, K. W. Kwon, and M. Shim,

*Nat. Phys.* **5**, 129 (2009).

<sup>19</sup>S. Morishita, J. Yamasaki, K. Nakamura, T. Kato, and N. Tanaka, *Appl. Phys. Lett.* **93**, 183103 (2008).

<sup>20</sup>P. D. Nellist, B. C. McCallum, and J. M. Rodenburg, *Nature (London)* **374**, 630 (1995).

<sup>21</sup>P. D. Nellist and J. M. Rodenburg, *Acta Crystallogr., Sect. A: Found. Crystallogr.* **54**, 49 (1998).

<sup>22</sup>J. M. Rodenburg and H. M. L. Faulkner, *Appl. Phys. Lett.* **85**, 4795 (2004).

<sup>23</sup>H. M. L. Faulkner and J. M. Rodenburg, *Phys. Rev. Lett.* **93**, 023903 (2004).

<sup>24</sup>W. Hoppe, *Acta Crystallogr.* **A25**, 495 (1969).

<sup>25</sup>J. M. Rodenburg, A. C. Hurst, and A. G. Cullis, *Ultramicroscopy* **107**, 227 (2007).

<sup>26</sup>J. M. Rodenburg, A. C. Hurst, A. G. Cullis, B. R. Dobson, F. Pfeiffer, O. Bunk, C. David, K. Jefimovs, and I. Johnson, *Phys. Rev. Lett.* **98**, 034801 (2007).

<sup>27</sup>P. Thibault, M. Dierolf, A. Menzel, O. Bunk, C. David, and F. Pfeiffer, *Science* **321**, 379 (2008).

<sup>28</sup>D. Gabor, *Nature (London)* **161**, 777 (1948).

<sup>29</sup>J. C. H. Spence, X. Zhang, and W. Qian, *Electron Holography* (Elsevier, New York, 1995), p. 267.

<sup>30</sup>A. M. Maiden and J. M. Rodenburg, *Ultramicroscopy* **109**, 1256 (2009).

<sup>31</sup>O. Bunk, M. Dierolf, S. Kynde, I. Johnson, O. Marti, and F. Pfeiffer, *Ultramicroscopy* **108**, 481 (2008).

<sup>32</sup>H. Lichte, in *Electron Holography*, edited by A. Tonomura (North-Holland, Amsterdam, 1995), p. 11.

<sup>33</sup>L. J. Allen, W. McBride, N. L. O'Leary, and M. P. Oxley, *Ultramicroscopy* **100**, 91 (2004).

<sup>34</sup>O. Kamimura, K. Kawahara, T. Doi, T. Dobashi, T. Abe, and K. Gohara, *Appl. Phys. Lett.* **92**, 024106 (2008).